Biochimie 242 (2026) 143–148

Contents lists available at ScienceDirect

Biochimie

journal homepage: www.elsevier.com/locate/biochi

Human mitochondrial persulfide dioxygenase is potently and reversibly inhibited by nitric oxide

Francesca Giordano [a], Diogo H.P. Silva [b], Elena Forte [a], Alessandro Giuffrè [a,c,*], João B. Vicente [b,**]

[a] Department of Biochemical Sciences, Sapienza University of Rome, I-00185, Rome, Italy
[b] Instituto de Tecnologia Química e Biológica António Xavier (ITQB NOVA), 2780-157, Oeiras, Portugal
[c] CNR Institute of Molecular Biology and Pathology, I-00185, Rome, Italy

ARTICLE INFO

Article history:
Received 6 September 2025
Received in revised form
6 December 2025
Accepted 3 January 2026
Available online 5 January 2026

Keywords:
Hydrogen sulfide
ETHE1
Sulfide detoxification pathway
Reactive sulfide species
Reactive nitrogen species
Crosstalk between gasotransmitters

ABSTRACT

Hydrogen sulfide (H_2S) regulates multiple human physiological processes, its reactivity and range of action being tightly controlled through regulation of H_2S-synthesizing and -detoxifying enzymes. H_2S detoxification is mainly achieved by a mitochondrial sulfide detoxifying pathway including persulfide dioxygenase (PDO). Human PDO (known as ethylmalonic encephalopathy protein 1, ETHE1), a homodimeric enzyme with a mononuclear iron centre active site, catalyzes the conversion of glutathione persulfide (GSSH) and O_2 to reduced glutathione (GSH) and sulfite. Here we report that ETHE1 is potently inhibited by authentic nitric oxide (NO) gas at physiological concentrations, as observed by high resolution respirometry. Inhibition is reversible, occurs via NO binding to the reduced mononuclear iron center and becomes more potent and persistent at lower O_2 levels. Incubation with *S*-nitrosoglutathione (GSNO) also appears to partially and transiently inhibit ETHE1, this effect likely resulting from *S*-nitrosation of cysteine residues. While ETHE1 is devoid of NO reductase activity, in aerobic conditions it displays low NO degrading activity. These findings unravel a novel layer of cross-regulation between the H_2S and NO gasotransmitters with possible implications on the regulation of numerous physiological and pathophysiological processes.

1. Introduction

Hydrogen sulfide (H_2S) plays a key role as a signaling molecule in human physiology and disease. To exert its function, H_2S interacts with several protein targets, either by transient binding at metal centers or promoting a reversible post-translational modification of cysteine residues designated as persulfidation. The number of proteins regulated by H_2S has been constantly growing, with implications not only for protein structure and function but also for human (patho)physiology.

H_2S is enzymatically produced by at least four different human enzymes [1]: cystathionine β-synthase (CBS), cystathionine γ-lyase (CSE), 3-mercaptopyruvate sulfurtransferase (MST), and selenium-binding protein 1 (SELENBP-1) [2]. In addition, non-enzymatic production can occur from reaction of free cysteine, iron and pyridoxal 5′-phosphate in plasma [3], and from decomposition of diet-derived polysulfides. Moreover, H_2S is also produced by the gut microbiota, mainly by dissimilatory sulfate reduction [4]. Given its reactivity and potential toxicity, disposal of H_2S is controlled by different enzymatic systems. A sulfide detoxification pathway comprising four enzymes locates to the mitochondria [5]. There, H_2S is oxidized by the membrane-associated sulfide:quinone oxidoreductase, which transfers electrons to quinone

Abbreviations: CBS, cystathionine β-synthase; CO, carbon monoxide; CSE, cystathionine γ-lyase; DTNB, 5,5′-dithiobis 2-nitrobenzoic; ETHE1, ethylmalonic encephalopathy protein 1; GSH, reduced glutathione; GSNO, *S*-nitrosoglutathione; GSSG, oxidized glutathione; GSSH, glutathione persulfide; H_2S, hydrogen sulfide; MST, 3-mercaptopyruvate sulfurtransferase; NaPi, sodium phosphate buffer; NO, nitric oxide; PBS, phosphate buffer saline; PDO, persulfide dioxygenase; SELENBP-1, selenium-binding protein 1.

* Corresponding author. CNR Institute of Molecular Biology and Pathology, Piazzale Aldo Moro 5, I-00185, Rome, Italy.
** Corresponding author. Instituto de Tecnologia Química e Biológica António Xavier, NOVA University of Lisbon, Avenida da República (EAN), 2780-157, Oeiras, Portugal.
E-mail addresses: alessandro.giuffre@cnr.it (A. Giuffrè), jvicente@itqb.unl.pt (J.B. Vicente).

https://doi.org/10.1016/j.biochi.2026.01.001

acceptors and a sulfur to reduced glutathione (GSH) as preferred substrate, thereby generating glutathione persulfide (GSSH). In the mitochondrial matrix, ETHE1 converts GSSH and O_2 to GSH and sulfite, while thiosulfate sulfurtransferase converts GSSH and sulfite to GSH and thiosulfate. Sulfite can eventually be oxidized to sulfate by sulfite oxidase in the intermembrane space. In addition, superoxide dismutase has recently been posited as an H_2S-detoxifying enzyme [6].

ETHE1 is a homodimeric metalloprotein of the metallo-β-lactamase structural family [7,8]. Each ~27 kDa-monomer binds a non-heme mononuclear iron ion, with His79, His135 and Asp154 as endogenous ligands and three hydroxo/aquo ligands. The mechanistic details underlying the persulfide dioxygenase (PDO) activity have been thoroughly investigated spectroscopically [9]. Until the recognition of its role in H_2S catabolism, human PDO was mostly known for its involvement in the rare inborn error of metabolism ethylmalonic encephalopathy (hence its designation as ethylmalonic encephalopathy protein 1, ETHE1) [10–13]. Currently, altered expression of ETHE1 has been associated with numerous pathologies, particularly cancer [14–16], cardiovascular [17] and inflammatory bowel diseases [18]. Moreover, oxidative post-translational modification of the enzyme has been found in association with brain aging in a mouse model [19].

Our groups have characterized the molecular mechanisms of several regulatory checkpoints of H_2S metabolism by the other two gasotransmitters, NO and carbon monoxide (CO). In particular, we have reported on the kinetics of CBS inhibition by NO and CO [20–22], and on the inhibitory effect of *s*-nitrosation on CSE [23]. These cross-regulatory mechanisms can have several physiological and pathophysiological implications and offer various possibilities for pharmacological interventions [24]. Herein we report on the inhibition of ETHE1 by NO and nitrosothiols, as investigated by high resolution respirometry and NO amperometry.

2. Materials and methods

2.1. Production and characterization of recombinant ETHE1

The recombinant mature form of ETHE1 was produced as described in Ref. [13]. Protein quantitation was determined by the Bradford method [25] and iron quantitation by the 3-(2-pyridyl)-5,6-bis(4-phenylsulfonic acid)-l,2,4-triazine (ferrozine) assay [26].

2.2. Preparation of hydrogen sulfide and glutathione persulfide solutions

Hydrogen sulfide solutions were prepared through an adaptation of the protocols described in Ref. [27]. Briefly, a crystal of $Na_2S•9H_2O$ (Sigma Aldrich 208043) was transferred to a sealed vial degassed by nitrogen flushing. The crystal was then dissolved into degassed 200 mM Tris/HCl buffer at pH 8.0, transferred anaerobically with a gas-tight Hamilton syringe. The resulting solution was protected from light and quantitated by the 5,5′-dithiobis 2-nitrobenzoic (DTNB) spectrophotometric method [28]. Glutathione persulfide (GSSH) solutions were prepared as an adaptation of the method described in Ref. [12]. Briefly, a solution of oxidized glutathione (GSSG) at 60 mM in 200 mM TrisHCl pH 8.0 was thoroughly degassed by nitrogen gas bubbling in a 10 mL gas-tight syringe. The H_2S solution was then added anaerobically to the GSSG-containing gas-tight syringe to yield final concentrations of 5 mM H_2S and 50 mM GSSG. The syringe was protected from light and incubated at room temperature for 1 h before being placed on ice. GSSH solutions were quantitated by cold cyanolysis as described in Ref. [29].

2.3. Preparation of NO and CO solutions

NO solutions were prepared by equilibrating in a tonometer thoroughly degassed milli-Q® water with pure NO gas at 1 atm and 20 °C. The NO solution was recovered from the tonometer in a 20 ml gas-tight syringe and kept sealed and protected from light. The NO concentration in solution was determined by titration of bovine cytochrome *c* oxidase, as described in Refs. [30,31]. CO solutions were prepared by bubbling CO at 1 atm and 20 °C in phosphate buffer saline (PBS) in a gas-tight syringe for 15–20 min, after which the syringe was sealed.

2.4. High resolution respirometry assays

O_2 consumption measurements were carried out at 25 °C in a high-resolution respirometer (Oxygraph-2K, Oroboros Instruments, Innsbruck, Austria). Assays were performed in 100 mM sodium phosphate (NaPi) buffer at pH 7.4, containing 130 $U{\cdot}mL^{-1}$ catalase (Sigma Aldrich C40) and 12 $U{\cdot}mL^{-1}$ SOD (Sigma Aldrich S7571). O_2 levels in the reaction mixture were adjusted by bubbling nitrogen gas into the buffer in the reaction chamber prior to closing the plungers. Typically, assays were initiated by addition of GSSH and catalytic amounts of ETHE1, prior to addition of any effector. Enzymatic activity was normalized to the catalytically active fraction of ETHE1 containing Fe. The maximal enzymatic activity was estimated from the initial oxygen consumption rate (OCR) upon addition of ETHE1 to the reaction chamber. Inhibition by NO was evaluated by adding aliquots of authentic NO solutions to ETHE1 in turnover with substrates, and estimating the decrease in oxygen consumption rate. To analyze the effect of *s*-nitrosation on persulfide dioxygenase activity, 10 μM ETHE1 was incubated with 0.5 mM *s*-nitrosoglutathione (GSNO; stock solutions prepared in 200 mM Tris-HCl pH 8.0 were quantitated spectrophotometrically) for 30 min at room temperature and protected from light, prior to addition to the reaction chamber. In control experiments with non-incubated ETHE1, GSNO (300 nM or 3 μM) was added to the reaction chamber to the enzyme in turnover with substrates. Data were collected at least in triplicates, unless stated.

2.5. NO consumption activity measurements

NO consumption activity assays were performed both in aerobic and anaerobic conditions by NO amperometry, interfacing an ISO–NO sensor probe connected to a TBR 4100 Free Radical Analyzer amplifier (both from World Precision Instruments) with the Oxygraph-2K high resolution respirometer. All assays were performed at 25 °C in 100 mM NaPi buffer at pH 7.4. In aerobic assays, a single bolus of ~5 μM NO was added to the reaction chamber (buffer containing 200 μM or 60 μM O_2, attained by purging the air-equilibrated buffer with nitrogen gas) containing 160 μM GSSH, in the absence or presence of 10 nM ETHE1. The aerobic NO consumption activity was estimated from the difference in NO decay rates (determined by fitting the data with a rise-and-fall kinetic model [32] in Graphpad Prism v 6.0) in the absence and presence of ETHE1.

NO reductase activity was assessed in anaerobic conditions. Briefly, the reaction buffer was thoroughly purged with nitrogen gas and strict anaerobic conditions were attained by addition of 5 mM sodium ascorbate and 10 $U{\cdot}mL^{-1}$ ascorbic oxidase. Following four sequential additions of NO stock solution, 80 μM GSSH was added, and subsequently ETHE1 was sequentially added twice (10 nM each). In control experiments, two additions of buffer were done at approximately the same time points at which the protein had been added. Data were collected at least in triplicates, unless stated.

3. Results and discussion

3.1. Glutathione persulfide dioxygenase activity of isolated recombinant ETHE1

GSSH dioxygenase activity of isolated recombinant ETHE1 was measured by high resolution respirometry (Fig. 1). Purified recombinant ETHE1 contained ~60 % of the expected Fe cofactor load. Similar values for Fe incorporation have been previously reported [33]. All enzymatic activity values were thus normalized to the catalytically active iron-loaded enzyme fraction.

Addition of GSSH alone elicited a slight increase in O_2 consumption rate (*not shown*), which suggests a slow auto-oxidation of GSSH, expectedly less evident at lower O_2 concentrations. Upon addition of ETHE1 (~6 nM), O_2 consumption was promptly elicited and followed close to 'zero-order' kinetics, as expected for steady-state conditions (Fig. 1A). At 160 μM GSSH and air-equilibrated O_2, persulfide dioxygenase activity was ~60 nM $O_2 \cdot s^{-1} \cdot$nM protein^{-1}, in line with the literature [12].

3.2. Inhibition of ETHE1 by authentic NO at physiological concentrations

Upon addition of authentic NO from a stock solution, ETHE1-catalyzed O_2 consumption rates immediately decreased, indicating enzyme inhibition by NO (Fig. 1A). Under standard assay conditions, starting from air-equilibrated buffer, the NO inhibition reached maximally ~60 %, and the enzyme partially recovered its activity with time (Fig. 1A, dashed lines). Under these conditions, by measuring the inhibition at different NO concentrations, an IC_{50} of 513 ± 26 nM for NO was estimated (Fig. 1B). ETHE1 inhibition by NO was assessed also at lower more physiological O_2 concentrations (starting from ~5 % of O_2 levels in air-equilibrated, Fig. 1A, solid lines). Notably, under such conditions, the inhibition was significantly stronger (maximal inhibition of ~80 %) and more persistent. At these lower O_2 concentrations, an IC_{50} of 70 ± 4 nM was estimated (Fig. 1B). Control experiments involving pre-incubation of GSSH with NO ruled out that the inhibitory effect resulted from GSSH depletion by NO (Supplementary Fig. S1).

3.3. Reactivity of ETHE1 towards NO

To further analyze the reactivity of ETHE1 towards NO, we resorted to NO amperometry to test the NO consumption activity in anaerobic or aerobic conditions. As observed in Supplementary Fig. S2, in the absence of O_2, addition of ETHE1 to NO in the presence of excess GSSH yielded no noticeable increase in NO decay, indicating that ETHE1 is devoid of NO reductase activity. Conversely, in aerobic conditions ETHE1 displayed a low NO degrading activity, as observed by comparing the kinetics of NO decay at different GSSH concentrations, in the absence or presence of ETHE1. As observed in Fig. 2A and B, the decay of NO added in bolus to the reaction mixture containing GSSH is slower in the absence (dotted lines) than in the presence (dashed lines) of 10 nM ETHE1. The extent of this difference inversely depends on the oxygen concentration (Fig. 2C).

3.4. Modulation of ETHE1 activity by GSNO

Given the unusually high number of non-disulfide cysteines (nine in total) in ETHE1, we investigated the possible functional impact of enzyme *s*-nitrosation following incubation with GSNO. As observed in Fig. 3A, GSNO-incubated ETHE1 (solid lines) appeared to be moderately inhibited (~30 %) with respect to the non-incubated enzyme (dashed lines). Inhibition was transient, being progressively lost after approximately 1 min, when the control O_2 consumption rate of the non-incubated enzyme was restored. To test whether the inhibitory effect derived from protein *s*-nitrosation, we further incubated GSNO-reacted ETHE1 with sodium ascorbate, which reverts *s*-nitrosation. As observed in Supplementary Fig. S3, ascorbate restored the ETHE1 enzymatic activity to ~90 % of the buffer-incubated enzyme, thereby confirming that the inhibition of GSNO-incubated ETHE1 results from protein *s*-nitrosation. Further, we investigated the effect of GSNO addition to ETHE1 in turnover with GSSH; GSNO indeed reacts with GSSH to yield NO [34,35]. Namely, we performed an experiment in which non-incubated ETHE1 was added to the assay, and then exogenous GSNO was added to the enzyme in turnover with substrates. As observed in Fig. 3B, addition of 300 nM (solid lines) or 3 μM (dashed lines) GSNO elicited a prompt inhibition with a very similar profile to that caused by NO, both in terms of extent and persistence of inhibition. We confirmed that this inhibition resulted from NO released upon reaction of GSNO with GSSH, as no ETHE1 inhibition was observed by performing the same experiment in the presence of oxyferrous myoglobin acting as a fast NO scavenger (Supplementary Fig. S4).

Altogether, these results indicate that there are two distinct mechanisms of ETHE1 functional control by NO and nitrosothiols. While ETHE1 is promptly inhibited by NO binding to the ferrous iron in the active site, one or more Cys residues could be *s*-

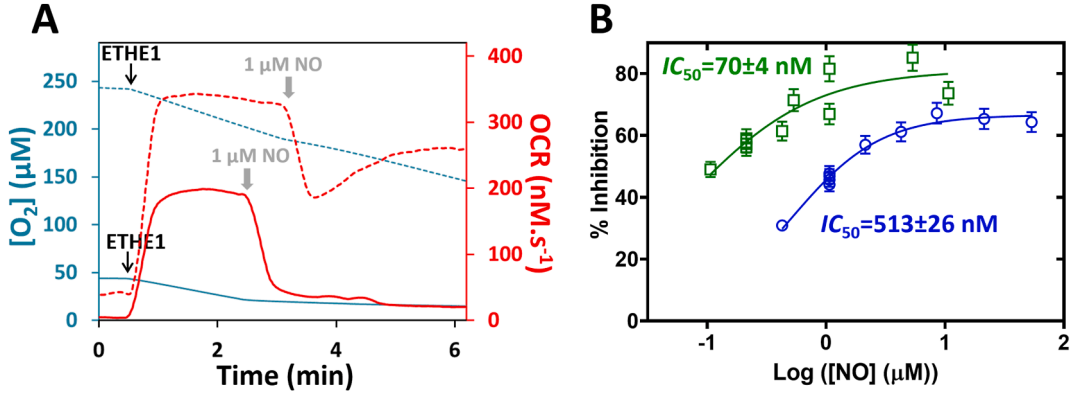

Fig. 1. Inhibition of ETHE1 by NO. *Panel A*, Representative traces of the effect of NO inhibition on ETHE1 activity at 25 μM O_2 (solid lines) and at 202 μM O_2 (dashed lines). Blue lines, O_2 concentration; red lines, O_2 consumption rates (OCR). *Panel B*, inhibition of ETHE1 activity as a function of NO concentration, measured at 25–32 μM O_2 (green squares) and 167–202 μM O_2 (blue circles). Error bars indicate uncertainty in OCR estimation. Data were fitted in Graphpad Prism (v6.0) with a log[inhibitor] vs. response – variable slope curve, yielding IC_{50} values of 70 ± 4 nM and 513 ± 26 nM at 25–32 μM O_2 and 167–202 μM O_2, respectively.

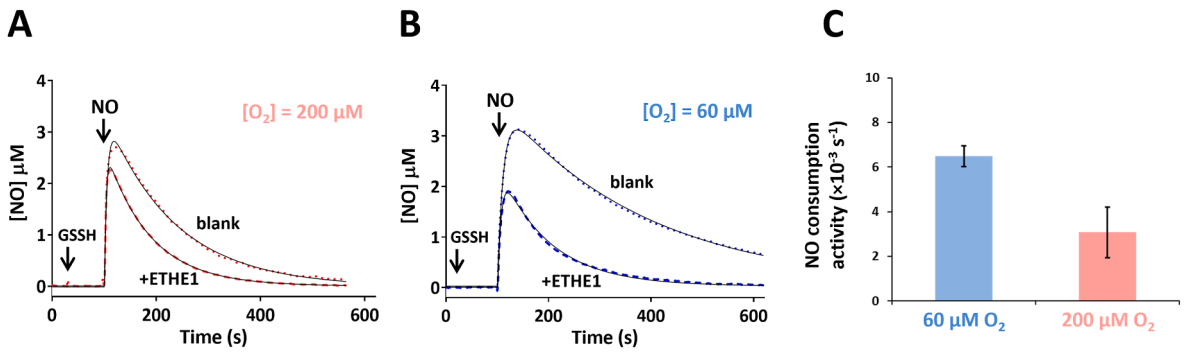

Fig. 2. NO consumption activity of ETHE1. NO consumption activity of ETHE1 assessed by NO amperometry. NO in bolus (~5 µM) promptly decays when added to oxygen-containing solutions (60 or 200 µM O_2) in the presence of GSSH and in the presence (+ETHE1, dashed lines) or absence (blank, dotted lines) of 10 nM ETHE1. *Panel A*, Representative trace of aerobic NO consumption of PDO activity in the presence of 160 µM GSSH and 200 µM O_2. *Panel B*, Representative trace of aerobic NO consumption activity of ETHE1 in the presence of 160 µM GSSH and 60 µM O_2. *Panel C*, Aerobic NO consumption activity measured at 60 µM O_2 (blue bar, $n = 2$) and 200 µM O_2 (pink bar, $n = 3$), calculated by fitting a rise-and-fall kinetics model with Graphpad Prism (v 6.0). Error bars correspond to standard uncertainty propagation for difference between independent terms: $SD_{net} = \sqrt{((SD_{+ETHE1})^2+(SD_{blank})^2)}$.

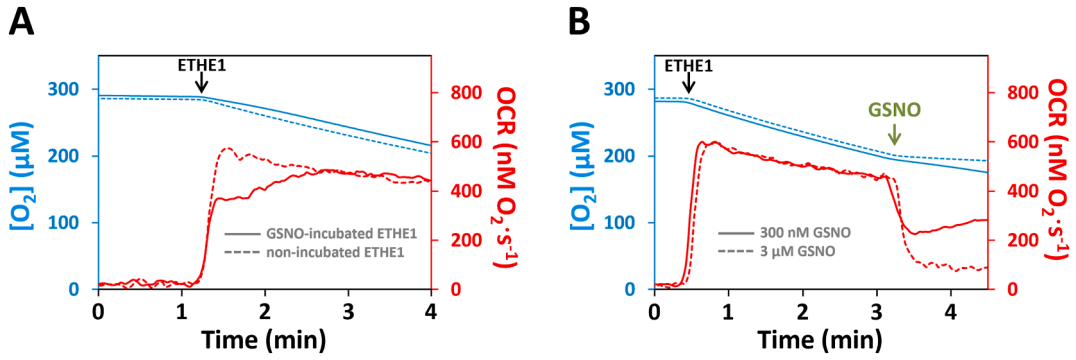

Fig. 3. Modulation of ETHE1 activity by GSNO. Functional impact of *S*-nitrosation on ETHE1 activity assessed by high resolution respirometry. Blue lines, O_2 concentration; red lines, O_2 consumption rates (OCR). Black arrow, addition of ETHE1. *Panel A*, Representative traces of the effect of GSNO pre-incubation on ETHE1 GSSH dioxygenase reaction. Solid lines, GSNO-incubated ETHE1; dashed lines, control with buffer-incubated ETHE1. *Panel B*, Representative traces of the effect of exogenously added GSNO (green arrow) to ETHE1 in turnover. Solid lines, 300 nM GSNO; dashed lines, 3 µM GSNO.

nitrosated upon incubation with GSNO, with a *per se* negative modulatory effect on ETHE1 function.

3.5. ETHE1 activity is unaffected by carbon monoxide, cyanide or thiosulfate

The ability of other effectors to modulate ETHE1 activity was also evaluated. Whereas NO had an inhibitory effect, CO, cyanide and thiosulfate were proven to be devoid of any modulatory activity towards ETHE1-catalyzed O_2 consumption (*not shown*). This observed selectivity for NO over other diatomic effectors like CO or CN^- clearly differentiates the chemical and structural properties of ETHE1 mononuclear non-heme iron active site from those of heme iron cofactors in various proteins, such as cytochrome *c* oxidase or human cystathionine β-synthase.

3.6. Mechanistic and pathophysiological implications

The ferrous nitrosyl (Fe–NO) adduct of ETHE1, as generated anaerobically by excess dithionite and mM amounts of the NO donor NONOate, was previously spectroscopically characterized [9]. This anaerobically stable adduct was employed to probe the binding mode of GSSH to the ferrous Fe, proposed to occur with two of the three water ligands respectively replaced by monodentate GSSH binding and NO. In the present study we showed that in ETHE1 at physiological levels of NO and O_2, the former is able to outcompete the latter for binding to ferrous Fe, thereby transiently inhibiting the persulfide dioxygenase activity of the enzyme (Fig. 4). The extent and persistence of inhibition are dependent both on the GSSH and O_2 concentration. Indeed, at low (<5 %) more physiological O_2 levels a more potent and persistent inhibition is established, reversed most likely by dissociation of NO from ferrous Fe. In addition, in the presence of O_2, ETHE1 was shown to display a slow NO degrading activity, although the products of this reaction remain to be determined.

These regulatory mechanisms for control of ETHE1 by NO constitute an addition to the growing list of reversible redox post-translational control of enzymes involved in H_2S metabolism. Indeed, modulation of H_2S production by NO and reactive nitrogen species has been reported for CBS [20–22,36–38] and CSE [23,39], with different physiological implications [40–45]. To our knowledge, this is the first report of control by NO of a human enzyme involved in H_2S catabolism, while thiosulfate sulfurtransferase had been shown to be inhibited by *S*-nitrosation [46]. In addition, GSSH transient accumulation due to ETHE1 inhibition may also impact the global protein persulfidation status, which can be either beneficial or harmful depending on the physiological context. Finally, the possibility of tuning mitochondrial H_2S consumption with NO affords a usefulness for NO-releasing drugs to pharmacologically address pathologies related with increased ETHE1 expression (e.g. Refs. [16–18]).

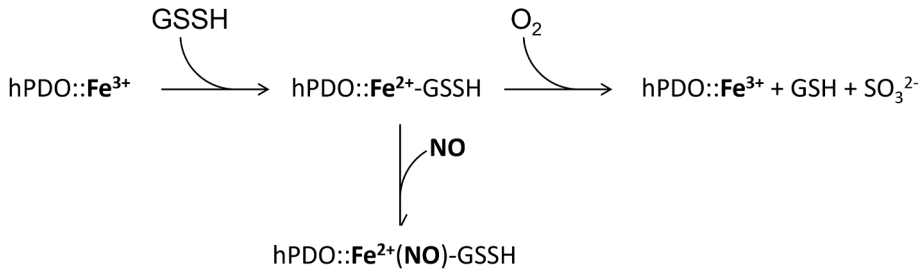

Fig. 4. Mechanism of human PDO inhibition by nitric oxide. In the canonic reaction, oxidized (hPDO::Fe^{3+}) is reduced by GSSH and ferrous PDO (hPDO::Fe^{2+}-GSSH) then reacts with oxygen to yield GSH and sulfite, returning to the ferric state. Upon reaction of hPDO::Fe^{2+}-GSSH with NO, the canonical reaction becomes inhibited.

CRediT authorship contribution statement

Francesca Giordano: Writing – review & editing, Investigation, Formal analysis. **Diogo H.P. Silva:** Writing – review & editing, Investigation, Formal analysis. **Elena Forte:** Writing – review & editing, Funding acquisition. **Alessandro Giuffrè:** Writing – review & editing, Project administration, Funding acquisition, Conceptualization. **João B. Vicente:** Writing – review & editing, Writing – original draft, Project administration, Investigation, Funding acquisition, Formal analysis, Conceptualization.

Declaration of competing interest

We have no conflict of interest to declare.

Acknowledgements

The Authors are thankful to Prof. Cláudio M. Gomes (Faculty of Sciences, University of Lisbon) for providing the plasmid for expression of ETHE1, and to João M. F. Costa for technical assistance with the enzyme purification. This work was partially supported by Fundação para a Ciência e a Tecnologia through iNOVA4Health (UIDB/04462/2020, UIDP/04462/2020), LS4FUTURE Associated Laboratory (LA/P/0087/2020), and by the Italian Ministry of University and Research with funds provided by the European Union within NextGenerationEU-MUR PNRR initiatives (PRIN 2022 grant 20224BYR59 to AG and EF and Extended Partnership initiative on Emerging Infectious Diseases - INF-ACT, Project no. PE00000007, to AG). JBV received support from Horizon 2020 project (MSCA-RISE-2018): ProMeTeus (ID: 823780).

Appendix A. Supplementary data

Supplementary data to this article can be found online at https://doi.org/10.1016/j.biochi.2026.01.001.

References

[1] O. Kabil, R. Banerjee, Enzymology of H2S biogenesis, decay and signaling, Antioxidants Redox Signal. 20 (2014) 770–782.
[2] E.B. Randi, G. Casili, S. Jacquemai, C. Szabo, Selenium-binding protein 1 (SELENBP1) supports hydrogen sulfide biosynthesis and adipogenesis, Antioxidants 10 (2021).
[3] J. Yang, P. Minkler, D. Grove, R. Wang, B. Willard, R. Dweik, C. Hine, Non-enzymatic hydrogen sulfide production from cysteine in blood is catalyzed by iron and vitamin B(6), Commun. Biol. 2 (2019) 194.
[4] F. Blachier, M. Andriamihaja, P. Larraufie, E. Ahn, A. Lan, E. Kim, Production of hydrogen sulfide by the intestinal microbiota and epithelial cells and consequences for the colonic and rectal mucosa, Am. J. Physiol. Gastrointest. Liver Physiol. 320 (2021) G125–G135.
[5] M. Libiad, P.K. Yadav, V. Vitvitsky, M. Martinov, R. Banerjee, Organization of the human mitochondrial hydrogen sulfide oxidation pathway, J. Biol. Chem. 289 (2014) 30901–30910.
[6] C.H. Switzer, S. Kasamatsu, H. Ihara, P. Eaton, SOD1 is an essential H(2)S detoxifying enzyme, Proc. Natl. Acad. Sci. U. S. A. 120 (2023) e2205044120.
[7] I. Pettinati, J. Brem, S.Y. Lee, P.J. McHugh, C.J. Schofield, The chemical biology of human Metallo-beta-Lactamase fold proteins, Trends Biochem. Sci. 41 (2016) 338–355.
[8] I. Pettinati, J. Brem, M.A. McDonough, C.J. Schofield, Crystal structure of human persulfide dioxygenase: structural basis of ethylmalonic encephalopathy, Hum. Mol. Genet. 24 (2015) 2458–2469.
[9] S. Goudarzi, J.T. Babicz Jr., O. Kabil, R. Banerjee, E.I. Solomon, Spectroscopic and electronic structure study of ETHE1: elucidating the factors influencing sulfur oxidation and oxygenation in mononuclear nonheme iron enzymes, J. Am. Chem. Soc. 140 (2018) 14887–14902.
[10] V. Tiranti, P. D'Adamo, E. Briem, G. Ferrari, R. Mineri, E. Lamantea, H. Mandel, P. Balestri, M.T. Garcia-Silva, B. Vollmer, P. Rinaldo, S.H. Hahn, J. Leonard, S. Rahman, C. Dionisi-Vici, B. Garavaglia, P. Gasparini, M. Zeviani, Ethylmalonic encephalopathy is caused by mutations in ETHE1, a gene encoding a mitochondrial matrix protein, Am. J. Hum. Genet. 74 (2004) 239–252.
[11] V. Tiranti, C. Viscomi, T. Hildebrandt, I. Di Meo, R. Mineri, C. Tiveron, M.D. Levitt, A. Prelle, G. Fagiolari, M. Rimoldi, M. Zeviani, Loss of ETHE1, a mitochondrial dioxygenase, causes fatal sulfide toxicity in ethylmalonic encephalopathy, Nat. Med. 15 (2009) 200–205.
[12] O. Kabil, R. Banerjee, Characterization of patient mutations in human persulfide dioxygenase (ETHE1) involved in H2S catabolism, J. Biol. Chem. 287 (2012) 44561–44567.
[13] B.J. Henriques, T.G. Lucas, J.V. Rodrigues, J.H. Frederiksen, M.S. Teixeira, V. Tiranti, P. Bross, C.M. Gomes, Ethylmalonic encephalopathy ETHE1 R163W/R163Q mutations alter protein stability and redox properties of the iron centre, PLoS One 9 (2014) e107157.
[14] M. Witherspoon, D. Sandu, C. Lu, K. Wang, R. Edwards, A. Yeung, O. Gelincik, G. Manfredi, S. Gross, L. Kopelovich, S. Lipkin, ETHE1 overexpression promotes SIRT1 and PGC1alpha mediated aerobic glycolysis, oxidative phosphorylation, mitochondrial biogenesis and colorectal cancer, Oncotarget 10 (2019) 4004–4017.
[15] X. Zhang, W. Dong, J. Zhang, W. Liu, J. Yin, D. Shi, W. Ma, A novel mitochondrial-related nuclear gene signature predicts overall survival of lung adenocarcinoma patients, Front. Cell Dev. Biol. 9 (2021) 740487.
[16] E. Ozluk, D. Coppola, I.Z. Mohammad, T. Islam, G. Ghali, C.G. Kevil, R.E. Shackelford, Ethylmalonic encephalopathy 1 protein is increased in colorectal adenocarcinoma, Anticancer Res. 41 (2021) 4719–4723.
[17] Z. Combi, L. Potor, P. Nagy, K.E. Sikura, T. Ditroi, E.P. Juranyi, K. Galambos, T. Szerafin, P. Gergely, M. Whiteman, R. Torregrossa, Y. Ding, L. Beke, Z. Hendrik, G. Mehes, G. Balla, J. Balla, Hydrogen sulfide as an anti-calcification stratagem in human aortic valve: altered biogenesis and mitochondrial metabolism of H(2)S lead to H(2)S deficiency in calcific aortic valve disease, Redox Biol. 60 (2023) 102629.
[18] N. Stummer, D. Weghuber, R.G. Feichtinger, S. Huber, J.A. Mayr, B. Kofler, D. Neureiter, E. Klieser, S. Hochmann, W. Lauth, A.M. Schneider, Hydrogen sulfide metabolizing enzymes in the intestinal mucosa in pediatric and adult inflammatory bowel disease, Antioxidants 11 (2022).
[19] P.J. Urrutia, D.A. Borquez, Expanded bioinformatic analysis of oximouse dataset reveals key putative processes involved in brain aging and cognitive decline, Free Radic. Biol. Med. 207 (2023) 200–211.
[20] J.B. Vicente, H.G. Colaco, F. Malagrino, P.E. Santo, A. Gutierres, T.M. Bandeiras, P. Leandro, J.A. Brito, A. Giuffre, A clinically relevant variant of the human hydrogen sulfide-synthesizing enzyme cystathionine beta-Synthase: increased CO reactivity as a novel molecular mechanism of pathogenicity? Oxid. Med. Cell. Longev. 2017 (2017) 8940321.
[21] J.B. Vicente, H.G. Colaco, P. Sarti, P. Leandro, A. Giuffre, S-Adenosyl-l-methionine modulates CO and NO* binding to the human H2S-generating enzyme cystathionine beta-synthase, J. Biol. Chem. 291 (2016) 572–581.
[22] J.B. Vicente, H.G. Colaco, M.I. Mendes, P. Sarti, P. Leandro, A. Giuffre, NO* binds human cystathionine beta-synthase quickly and tightly, J. Biol. Chem. 289 (2014) 8579–8587.
[23] D.G.F. Fernandes, J. Nunes, C.S. Tome, K. Zuhra, J.M.F. Costa, A.M.M. Antunes, A. Giuffre, J.B. Vicente, Human cystathionine gamma-Lyase is inhibited by s-Nitrosation: a new crosstalk mechanism between NO and H(2)S, Antioxidants 10 (2021).
[24] A. Giuffre, J.B. Vicente, Hydrogen sulfide biochemistry and interplay with

other gaseous mediators in mammalian physiology, Oxid. Med. Cell Longev. 2018 (2018) 6290931.
[25] M.M. Bradford, A rapid and sensitive method for the quantitation of microgram quantities of protein utilizing the principle of protein-dye binding, Anal. Biochem. 72 (1976) 248–254.
[26] L. Stookey, Two New Spectrophotometric Reagents for Copper *Talanta*, 17, 1970, pp. 644–647.
[27] P. Nagy, Z. Palinkas, A. Nagy, B. Budai, I. Toth, A. Vasas, Chemical aspects of hydrogen sulfide measurements in physiological samples, Biochim. Biophys. Acta 1840 (2014) 876–891.
[28] A.S. Nashef, D.T. Osuga, R.E. Feeney, Determination of hydrogen sulfide with 5,5'-dithiobis-(2-nitrobenzoic acid), N-ethylmaleimide, and parachloromercuribenzoate, Anal. Biochem. 79 (1977) 394–405.
[29] R. Greiner, T.P. Dick, Real-time assays for monitoring the influence of sulfide and sulfane sulfur species on protein thiol redox states, Methods Enzymol. 555 (2015) 57–77.
[30] A. Giuffre, P. Sarti, E. D'Itri, G. Buse, T. Soulimane, M. Brunori, On the mechanism of inhibition of cytochrome c oxidase by nitric oxide, J. Biol. Chem. 271 (1996) 33404–33408.
[31] G. Stubauer, A. Giuffre, M. Brunori, P. Sarti, Cytochrome c oxidase does not catalyze the anaerobic reduction of NO, Biochem. Biophys. Res. Commun. 245 (1998) 459–465.
[32] S.R.J. Hoare, P.H. Tewson, A.M. Quinn, T.E. Hughes, L.J. Bridge, Analyzing kinetic signaling data for G-protein-coupled receptors, Sci. Rep. 10 (2020) 12263.
[33] P. Ruhl, P. Haas, D. Seipel, J. Becker, A. Kletzin, Persulfide dioxygenase from acidithiobacillus caldus: variable roles of cysteine residues and hydrogen bond networks of the active site, Front. Microbiol. 9 (2018) 1610.
[34] J.M. Fukuto, C. Perez-Ternero, J. Zarenkiewicz, J. Lin, A.J. Hobbs, J.P. Toscano, Hydropersulfides (RSSH) and nitric oxide (NO) signaling: possible effects on S-Nitrosothiols (RS-NO), Antioxidants 11 (2022).
[35] C.L. Bianco, T.A. Chavez, V. Sosa, S.S. Saund, Q.N.N. Nguyen, D.J. Tantillo, A.S. Ichimura, J.P. Toscano, J.M. Fukuto, The chemical biology of the persulfide (RSSH)/perthiyl (RSS.) redox couple and possible role in biological redox signaling, Free Radic. Biol. Med. 101 (2016) 20–31.
[36] S. Taoka, R. Banerjee, Characterization of NO binding to human cystathionine beta-synthase: possible implications of the effects of CO and NO binding to the human enzyme, J. Inorg. Biochem. 87 (2001) 245–251.
[37] S. Carballal, E. Cuevasanta, P.K. Yadav, C. Gherasim, D.P. Ballou, B. Alvarez, R. Banerjee, Kinetics of nitrite reduction and peroxynitrite formation by ferrous heme in human cystathionine beta-synthase, J. Biol. Chem. 291 (2016) 8004–8013.
[38] C. Gherasim, P.K. Yadav, O. Kabil, W.N. Niu, R. Banerjee, Nitrite reductase activity and inhibition of H(2)S biogenesis by human cystathionine ss-synthase, PLoS One 9 (2014) e85544.
[39] C. Luo, D. Ji, Y. Li, Y. Cao, S. Zhang, W. Yan, K. Xue, J. Chai, Y. Wu, H. Liu, W. Wang, Abnormal nitration and S-sulfhydration modification of Sp1-CSE-H(2)S pathway trap the progress of hyperhomocysteinemia into a vicious cycle, Free Radic. Biol. Med. 164 (2021) 20–33.
[40] T. Hishiki, T. Yamamoto, T. Morikawa, A. Kubo, M. Kajimura, M. Suematsu, Carbon monoxide: impact on remethylation/transsulfuration metabolism and its pathophysiologic implications, J. Mol. Med. (Berl.) 90 (2012) 245–254.
[41] B. Kawahara, S. Ramadoss, G. Chaudhuri, C. Janzen, S. Sen, P.K. Mascharak, Carbon monoxide sensitizes cisplatin-resistant ovarian cancer cell lines toward cisplatin via attenuation of levels of glutathione and nuclear metallothionein, J. Inorg. Biochem. 191 (2019) 29–39.
[42] B. Kawahara, S. Sen, P.K. Mascharak, Reaction of carbon monoxide with cystathionine beta-synthase: implications on drug efficacies in cancer chemotherapy, Future Med. Chem. 12 (2020) 325–337.
[43] A.L. King, D.J. Polhemus, S. Bhushan, H. Otsuka, K. Kondo, C.K. Nicholson, J.M. Bradley, K.N. Islam, J.W. Calvert, Y.X. Tao, T.R. Dugas, E.E. Kelley, J.W. Elrod, P.L. Huang, R. Wang, D.J. Lefer, Hydrogen sulfide cytoprotective signaling is endothelial nitric oxide synthase-nitric oxide dependent, Proc. Natl. Acad. Sci. U. S. A. 111 (2014) 3182–3187.
[44] T. Morikawa, M. Kajimura, T. Nakamura, T. Hishiki, T. Nakanishi, Y. Yukutake, Y. Nagahata, M. Ishikawa, K. Hattori, T. Takenouchi, T. Takahashi, I. Ishii, K. Matsubara, Y. Kabe, S. Uchiyama, E. Nagata, M.M. Gadalla, S.H. Snyder, M. Suematsu, Hypoxic regulation of the cerebral microcirculation is mediated by a carbon monoxide-sensitive hydrogen sulfide pathway, Proc. Natl. Acad. Sci. U. S. A. 109 (2012) 1293–1298.
[45] G.A. Prathapasinghe, Y.L. Siow, Z. Xu, K. O, Inhibition of cystathionine-beta-synthase activity during renal ischemia-reperfusion: role of pH and nitric oxide, Am. J. Physiol. Ren. Physiol. 295 (2008) F912–F922.
[46] I. Kwiecien, M. Sokolowska, E. Luchter-Wasylewska, L. Wlodek, Inhibition of the catalytic activity of rhodanese by S-nitrosylation using nitric oxide donors, Int. J. Biochem. Cell Biol. 35 (2003) 1645–1657.